Chemical fingerprints for $PM_{2.5}$ in the ambient air near a raw material storage site for iron ore, coal, limestone, and sinter

Kavita Justus Mutuku[1,2], Yen-Yi Lee,[1,2,*], Guo-Ping Chang-Chien[1,2], Sheng-Lun Lin[3], Wei-Hsin Chen [4,5,6,*]

1. Super micro mass research and technology center, Cheng Shiu University, Kaohsiung 833, Taiwan.
2. Center for Environmental Toxin and Emerging-Contaminant Research, Cheng Shiu University, Kaohsiung 833, Taiwan.
3. School of Mechanical Engineering, Beijing Institute of Technology, Beijing 100081, China.
4. Department of Aeronautics and Astronautics, National Cheng Kung University, Tainan 701, Taiwan.
5. Research Center for Smart Sustainable Circular Economy, Tunghai University, Taichung 407, Taiwan.
6. Department of Mechanical Engineering, National Chin-Yi University of Technology, Taichung 411, Taiwan.

* Corresponding authors; E-mail: leeyenyi@gcloud.csu.edu.tw (Y.Y. Lee); chenwh@mail.ncku.edu.tw; weihsinchen@gmail.com (W.H. Chen)

Abstract

To understand the contributions of a raw material storage site for iron ore, coal, limestone, and sinter to the ambient air fine particulate matter ($PM_{2.5}$), the concentrations and chemical fingerprints for resuspended and ambient air $PM_{2.5}$ were compared. Investigations were done for 15 piles of raw materials including 5 iron piles, 5 coal piles, 3 stone piles, and a single pile each for coke and sinter. Additionally, four sites including sites A, B, C, and D in the surrounding of the storage site were chosen to investigate the ambient air $PM_{2.5}$. The concentrations, compositions, and i and j values for $PM_{2.5}$ varied significantly by season and in the four sites under investigation. The chemical fingerprints of the $PM_{2.5}$ show that water-soluble ions were the most important component in all sites. Specifically, SO_4^{2-} and NO_3^- were the predominant water-soluble ions in winter and summer respectively. The most dominant components in the iron ore, coal, limestone, coke, and sinter piles were iron, carbon, Ca^{2+} and carbon, carbon and SO_4^{2-}, and Fe and Ca^{2+}, respectively. During the summer, $PM_{2.5}$ concentrations ranged from 13.7~ 18 μg m^{-3}, the chemical composition of water-soluble ions, metals, carbon accounted for 54.2%, 5.70%, and 23.7% respectively. During winter, the concentrations ranged from 44.7 ~ 48. μg m^{-3}, the water-soluble ions, metals, carbon components accounted for 49.2%, 8.09%, and 17.4% respectively. From the chemical mass balance, the main sources of $PM_{2.5}$ in sites B, C, and D are stationary sources, mobile sources, and secondary organic aerosols. To effectively solve the air pollution menace associated with the surroundings of the raw material storage site, the environmental protection agency should formulate measures to effectively reduce the contribution of resuspended dust and other pollution sources to ambient air $PM_{2.5}$.

Keywords: $PM_{2.5}$; Chemical fingerprints; raw materials; re-suspension; seasonal variation.

Introduction

Deteriorating air quality caused by elevated concentrations of fine particulate matter ($PM_{2.5}$) from the raw material storage site for iron ore, coal, limestone, and sinter is a great cause of concern to the residents in the southern region of Taiwan. In the steel production industry, $PM_{2.5}$ is emitted during manufacturing as well as the resuspension process at the raw material storage sites. The iron ore sintering process for steel plants needs several materials including iron ore, coal, limestone, coke, and recycled steel (Fernández-González et al., 2017). Contingent to the particle size distribution and chemical compositions, the concentrations of $PM_{2.5}$ differ among piles of raw materials. Recently, existing plants have expanded their production due to increased demand for steel (Cullen et al., 2012). Consequently, information published by the Taiwan Emission database system (TEDS 9.0) shows that the steel industry is responsible for 15.9% of the total $PM_{2.5}$ emitted nationwide.

There are natural and anthropogenic sources of $PM_{2.5}$. However, emissions from the latter are believed to impact human health more adversely (Artíñano et al., 2003; Weijers et al., 2011). Major anthropogenic sources of fine particulates are associated with activities of modern industrialization such as combustion, construction, manufacturing processes, and road dust (de la Campa et al., 2010; Benchrif et al., 2018). A comparison study between the pollution contributions from long-range transportation from neighboring China and those from local sources in cities within Taiwan established that the later was more dominant (Lai and Brimblecombe, 2020).

Previous analyses of $PM_{2.5}$ in Taiwan indicate several compositions including, organic and elemental carbon, metals, crust elements, and water-soluble ions (Wang et al., 2020). Metallic compositions of $PM_{2.5}$ from industrial processes are not easily removed by the pollution control devices. Consequently, they end up being discharged into the atmosphere (Ahmad et al., 2018). Previously, surveys on the concentrations of metal components in particulate matters were conducted for six air quality monitoring stations including Nanzi, Zuoying, Sanmin, Qianjing, Qianzheng, and Xiaogang.

59 The metal components found included Al, Ca, Fe, and K. Overall, Fe was the most abundant metal and
60 Xiaogang station had the highest concentration (Lin et al., 2008; She et al., 2020).

61 Research on $PM_{2.5}$ is mostly focused on four processes including, emission, transformation,
62 transportation, and deposition (Pöschl, 2005; Choi et al., 2007; Shen et al., 2020). The latter is critical
63 to the human population since it directly impacts their health. It can be divided into wet and dry
64 deposition. In a wet deposition, the constituents of $PM_{2.5}$ are washed by precipitation culminating on
65 solid surfaces such as land and vegetation or in water masses such as lakes, rivers, and oceans (Zhao et
66 al., 2018). Through dry deposition, fine particulates wind up on surfaces or in the human or animal
67 lungs during inhalation (Zhang et al., 2014). Researchers have established reliable methods for sample
68 collection and quantification of particulate matter. Loo et al. (1975) describe the application of a
69 dichotomous sampler to collect fine and coarse particulate matter. Receptor models for connecting the
70 ambient air $PM_{2.5}$ and their emission sources were developed and applied in many studies (Houck,
71 1991; Pace, 1991; Wienke et al., 1994).

72 Inhalation of $PM_{2.5}$ has been linked to several adverse health effects of the respiratory system
73 including inflammation, cancer, and exacerbation of pre-existing respiratory conditions (Chalupa et al.,
74 2004; Feng et al., 2016). Additional adverse health effects to the rest of the human body include the
75 destruction of the nervous system, circulatory systems, aggravation of diabetes mellitus, and anomalies
76 to newborns (Nogueira, 2009; Zhao et al., 2013). Several $PM_{2.5}$ compositions including, Ca, black
77 carbon, V, and Zn are associated with cardiovascular hospitalization while road dust, sea salt,
78 aluminium, calcium, chlorine, black carbon, nickel, silicon, titanium, and vanadium. are linked to
79 respiratory complications (Bell et al., 2014). According to a study by Dejmek et al., (1999), the odds
80 ratio for intrauterine growth retardation upon exposure of pregnant mothers to $PM_{2.5}$ was 1.26.
81 Additionally, women with high pre-pregnancy exposure to $PM_{2.5}$ experienced increased incidences of
82 gestational diabetes mellitus (Monshi and Asgarani, 1999).

In the study of emission sources for particulates, resuspension which is the removal of initially deposited material by a mechanical process such as wind, traffic, and soil cultivation is rarely covered. Resuspended $PM_{2.5}$ can be transported to residential areas and rise to the level coinciding with the average breathing zone hence posing an inhalation exposure risk to the residents. Herein, the chemical fingerprints of resuspended $PM_{2.5}$ from a raw material storage site and its contribution to ambient $PM_{2.5}$ in the surrounding area were investigated. A receptor model called chemical mass balance (CMB) was applied to estimate the contribution of different pollution sources to ambient $PM_{2.5}$. To the authors' knowledge, a study on the contribution of resuspended particles from the raw material storage site to ambient air $PM_{2.5}$ has not been carried out before. Therefore, this study can fill in the research gap and provide useful insights into developing pollution control strategies for the affected emission sources. Gathering comprehensive knowledge of emission sources and chemical compositions of $PM_{2.5}$ in the surroundings of the storage site is an appropriate step towards understanding the overall air quality to build proper health guidelines for the residents in the neighborhood.

Methodology

Sample collection at the raw material storage field and its surroundings

The area under investigation was separated into 4 sites, herein referred to as sites A, B, C, and D as shown in **Fig. 1**. Site A encompasses the raw material storage zone. Sites B and C are densely populated areas next to the raw material storage site. Site D is also densely populated but further from the raw material storage site compared to sites B and C. Samples were collected at the raw material storage site for three days in each season to represent summer and winter. The sampling dates for the two seasons were on 5^{th}, 8^{th}, and 11^{th} in August for summer and 9^{th}, 15^{th}, and 27^{th} in December for Winter. Sampling dates were synchronized with the dates of $PM_{2.5}$ manual inspections for the EPA monitoring station. Additionally, a peripheral airborne particulate sampler (BGI PQ200) was applied to collect samples continuously for 24 hours.

A total of 15 samples were collected to represent each of the following, 5 piles of irons ore (Iron ore 1~5), 5 piles of coal (coal pile 1~5), 3 piles of limestones (limestone 1~3), 1 pile each of sinter and coke. Special care was taken to adhere to the soil sampling method (S102.63B) announced by the national institute of Environmental Analysis (NIEA). The topsoil samples were divided into composites and grab samples. Samples from different sampling points on the horizontal surface were mixed to obtain the average concentration for that specific area. A virtual grid was applied to collect the samples at the intersections as well as within the grids.

The soil samples were obtained and put in separate plastic lock bags. Reagents used for the treatment of the soil samples include phosphate-free detergent, distilled water, acetone, and n-hexane. Decontamination of the sampling equipment was performed between the collection of consecutive samples. A metal brush was used to remove debris from the equipment, a non-phosphorus detergent was applied on a brush after-which the device was brushed thoroughly before rinsing with distilled water and then with organic solvents (acetone or n-ethane). Lastly, the sampling device was rinsed with distilled water.

Re-suspension tests

After obtaining the coarse and fine particulate matters from the sample (PM_{10} and $PM_{2.5}$) a resuspension test was performed. The resuspension chamber was carefully constructed and set to accurately represent natural wind. A resuspension system was used to administer tests to determine both the vertical and lateral translocation of fine particulates within the enclosed space. The re-suspension test was performed for the portion of total suspended solids (TSP) that passed through the 400-mesh size ($D < 38$ μm) and reached the bottom plate. The powder was collected in a stainless-steel dish and then loaded into a dry powder generator. An accelerated airflow rate of 16.7 L min^{-1} was applied to simulate natural wind in the re-suspension chamber. A dichotomous sampler for PM_{10} and $PM_{2.5}$ was used to collect coarse and fine particulate matter. The re-suspension chamber had a 1 m

square horizontal cross-section and a height of 2 m. A dichotomous sampler was placed under the re-suspension chamber**.** The total time for re-suspension and sample collection was 5 minutes.

Weighing and conditioning of the samples

A microbalance was used for the 24 filter paper samples. The inspection was done for each sampling filter paper using a lamp and a magnifying glass to confirm the integrity of the filter paper. The following factors were considered to compromise the integrity of the filter paper including breakage, indentation, dent, scratch, fiber, and particle contamination. Care was taken to preserve the integrity of the filter paper during unpackaging, weighing, conditioning, and clipping. The filter paper was then placed in a conditioning environment for 12 hours. This was succeeded by fine weighing. The steps of conditioning and fine weighing were repeated until the difference in weight was constant and less than 5 µg. The average of the weight before and after conditioning was taken as the weight after sampling. The formula for the calculation of $PM_{2.5}$ concentration is as follows;

$$PM_{2.5}\ Concentration = \frac{W_f - W_i}{V_a} \quad (1)$$

where $PM_{2.5}$ concentration is in µg m^{-3}. W_i and W_f represent the masses of the filter paper in µg before and after sampling respectively. V_a is the total volume of air in m^3.

To collect samples for ambient air $PM_{2.5}$, blank filter papers are exposed to the atmosphere for 24 hours and with a sample volume of 24 m^3. The detection limit is 2 µg m^{-3}.

Analysis of metal compositions, water-soluble ion components, and carbon content

Evaluating the chemical fingerprints for $PM_{2.5}$, involved establishing their metal components, water-soluble ion concentration, and carbon content. A total of 15 were tested for 31 metal elements including Li, Be, Na, Mg, Al, K, Ca, Ti, V, Cr, Mn, Fe, Co, Cu, Zn, Ga, As, Se, Rb, Sr, Ag, Cd, In, Sn, Cs, Ba, Tl, Pb, U, Ni, and Si. Further analyses were done for 4 anionic species including SO_4^{2-}, NO^-, CI^-, F^-, and 5 cationic species including Na^+, K^+, Ca^{2+}, Mg^{2+}, NH_4^+. The concentrations of elemental and organic carbons (EC and OC) were evaluated.

The metal compositions analysis for $PM_{2.5}$ was performed using the other half of the Teflon filter paper. The microwave digestion pretreatment process established by the environmental protection administration (EPA) was applied. First, calibration was done using 5 standard solutions to produce a calibration line. The relative error value of the calibration line should be within ±10%. Otherwise, the operating condition of the instrument must be checked or maintenance must be performed and another calibration line must be developed. After calibration, the samples were put into ICP/MS for analysis. The blank sample must not exceed double the MDL. A blank sample is prepared and analyzed after every 10 samples. Care was taken to ensure a recovery rate of 80~120%. Further one sample was tested twice in every batch of 10 samples. The relative difference between the two measurements must not exceed 20%. Quantification of the metal composition in the $PM_{2.5}$ samples was performed by high-resolution inductively coupled plasma in series with a mass spectrometer (ICP-MS, Agilent 7500A). The calibration line was checked by standard solution whereby the acceptable absolute error should be less than 10%.

Sample pretreatment involved shaking half of each collected Teflon filter using ultrasonic vibrations for 90 minutes in 10 mL of deionized water. After extraction, the 10 mL was poured into a syringe and filtered with a 0.45 μm membrane to remove particles. Quantification of the water-soluble anions was performed using an Ion Chromatograph (IC) (Dionex, Model DX-120) series conductivity detector. Analysis of the anions was performed using a with ASRS-ULTRA suppressor, Ion Pac AS4A-SC column, and Na_2CO_3/$NaHCO_3$ eluent. On the other hand, cations were evaluated using CSRS-ULTRA suppressor, Ion Pac CS12 column, and 0.1 M H_2SO_4 eluent. The concentrations in blank samples fell below the limit of detection (LOD) for all ions. Therefore, deductions were unnecessary for the calibration data.

An elemental analyzer (Elementar Vario MIRCO Cube), with the AS 200 type Autosampler and DP 700 integrator for were used to quantify both the EC and OC. The equipment's precision and stability are shown in **Table 1** while its operating conditions are in **Table 2.** A quartz filter paper was

first placed in the thermal chamber and heated to 900 °C to remove any available carbon before chemical analysis. Analysis of the carbon content in $PM_{2.5}$ applies the instantaneous dynamic oxidation. The sample's chemical bonds are broken in the quartz reaction tube. It is rapidly oxidized to CO_2 after which it is reduced using Cu and then passed through the separation column for detection using a thermal conductivity detector (TCD). The organic carbon content is obtained by the difference between total carbon (TC) and EC.

Chemical mass balance

The chemical mass balance was applied for the nearby emission sources including, the raw material storage site, background soil dust, traffic dust, mobile sources, steel industry, various industrial boilers, electric arc furnaces, coke ovens, sintering furnaces, Power plants, and incinerators as shown in **Table 1**. Criteria for the selection of emission sources included chi-square value of less than 4.0, press normalization $R^2 > 0.8$, T statistic (ratio of contribution of the sources and the standard errors) >2.0, the ratio of the calculated to the measured value should be 0.8 ~1.2, (preferably close to 1.0), residual and uncertainty ratio should be -2.0 ~ 2.0 (preferably 0), unquantified and similar clusters should be preferably absent and better Degrees of Freedom.

The theory of the receptor model is based on the similarities between the chemical compositions of the emission sources and those of the receptor sites. It is supported by the principle of conservation of mass and statistics. The pollutant concentration at the receptor point is the linear summation of the pollution sources. The main simplifying assumption is that there are no chemical reactions between different chemical species from the emission sources. A fingerprint database required for the chemical mass balance receptor model was established before the CMB8.2 receptor model was applied to estimate the respective percentage contributions of the $PM_{2.5}$ sources to ambient air $PM_{2.5}$.

Results and discussion

Ambient air $PM_{2.5}$ concentration during summer and winter.

Kaohsiung has a tropical climate whereby rainfall is experienced in 5-9 months of the year. The average annual temperature is about 24.3 °C while the annual rainfall is about 1738 mm (Chen and Chen, 2003). During summer warm and humid air masses flow from the southern side which is mostly ocean. During moments of rainfall and typhoon, the relative humidity ranges between 69.85 and 74.76%. Wind flow over the Kaohsiung region leads to the lower relative humidity in winter which ranges between 67.51 and 70.60%.

From the year 2005 to 2017, the EPA has been comparing manually calculated hourly concentrations for $PM_{2.5}$ to the ones from the automatic monitoring station. The $PM_{2.5}$ annual average concentration for 13 years is presented in **Fig. 2**. There has been a steady decrease in the concentration of $PM_{2.5}$ in Xiaogang station from 55.2 μg m^{-3} in 2005 to 36.2 μg m^{-3} in 2017. Similarly, in Daliao, the concentrations were 50.4 and 3.02 μg m^{-3} in the respective years. The reduction over the period was 34.4% and 40.1% for Xiaogang and Daliao stations respectively. The Taiwan EPA has put control measures to reduce the emission for air pollutants including $PM_{2.5}$, PM_{10}, SO_x, NO_x and NMHC from both mobile and stationary sources. This could explain the trend for $PM_{2.5}$ in Xiaogang and Daliao for the years 2005~2017. The variations in the $PM_{2.5}$ concentration in winter and summer can be explained by the north and south winds which are dominant during winter and summer respectively (Tsai et al., 2003). During winter, the dominance of the north wind reduces the possibilities of vertical diffusion of $PM_{2.5}$ in the mixed layer.

The $PM_{2.5}$ concentration in summer ranges from 13.7-18.0 μg m^{-3} as shown in **Fig. 3**. This is below the 24 -hour standard in Taiwan. The proportion of water-soluble ions is the highest, with an average of 7.4 and 22.7 μg m^{-3} in summer and winter respectively of the total $PM_{2.5}$ mass. In summer, the carbon composition by mass exceeded the contribution from other chemicals in site C only. However, in winter, the concentration of other chemicals exceeded that of the carbon contents in all sites. The average carbon content was 11.8% and 34.2% in summer and winter respectively. The mass

composition in winter exceeded that of summer because of lower wind recirculation and hence limited dilution rates (Virtanen et al., 2006; Tseng et al., 2019). The average mass concentrations of EC and OC in the atmospheric $PM_{2.5}$ for summer and winter seasons for the 4 sites under investigation are shown in **Fig. 4**. The seasonal average OC content ranges between 1.2 and 3.0 μg m^{-3} in summer while the range for summer is between 5.6 to 6.2 μg m^{-3}. EC content's range is wider for summer than for winter. In summer, it ranges from 0.6 to 1.8 μg m^{-3} while in winter it ranges from 1.7 to 2.2 μg m^{-3}. EC is emitted from the incomplete combustion of fuels while OC results from the degradation of carbonaceous materials. The dominance of either EC or OC indicates the major source of carbonaceous aerosols.

Carbonaceous aerosols form a major component of PM and play a major role in atmospheric chemistry. Investigations carried out in the past, found that the $\frac{OC}{EC}$ in the region ranged between 2.32 and 2.76 in periods when the sea and land breeze interacted (Fang et al., 2008). Herein the $\frac{OC}{EC}$ ratio ranged between 1.5 to 4.0. This indicates that the predominant sources of carbon content in $PM_{2.5}$ are photochemical reactions, industrial and combustion processes. This is in line with previous studies on carbon compositions in $PM_{2.5}$ in the Kaohsiung metropolitan area. For instance, Huang (1991) found that carbon content accounted for about 22.1% of the ambient air $PM_{2.5}$ on average, and the average $\frac{OC}{EC}$ ratio was 2.6. The $\frac{OC}{EC}$ ratio can be applied to determine the intensity of secondary organic aerosol formation. The critical value is $\frac{OC}{EC}$ =2.2 or $\frac{OC}{TC}$=0.67. Carbon component analysis methods include thermal decomposition method (TM), solvent extraction (SEM), thermal manganese oxidation method (TMO), thermo-optical reflection method (TOR) optics, and thermo-optical transmission method (TOT). For sites A, B, and C, during summer the $\frac{OC}{EC}$ value is less than 2.2 indicating a low potential for the formation of secondary organic aerosols (SOA). In summer, the $\frac{OC}{EC}$ for Site D greatly exceeds that from the other sites. This is because site D is a rural area and therefore, the degradation of carbon-

containing products such as vehicle tires and vegetation dominates emits more carbonaceous aerosols compared to incomplete combustion of carbon-containing fuels.

In the other times the $\frac{OC}{EC}$ ratio in all sites during winter exceeds 2.2 indicating a high potential for the formation of SOA (Pandis et al., 1992; Cao et al., 2008). Overall, carbonaceous $PM_{2.5}$ are mainly emitted from combustion sources upwind of the site under investigation including mobile sources and fixed sources such as the petrochemical industry, boilers, steelmaking process, and secondary derived aerosols.

Chemical speciation of ambient air $PM_{2.5}$

The concentrations of $PM_{2.5}$ and their speciation at the sites under investigation for two seasons are presented in **Fig. 3**. The concentration during winter exceeds that of summer for all sites. Further, it can be observed that metals had the lowest concentration in all sites and for all seasons. The most important category of chemicals is water-soluble ions. Site B has the highest metal composition while site D had the lowest concentration of metals and water-soluble ions. This phenomenon can be attributed to the proximity of the respective sites to the raw material storage site and the dominant wind directions (Cohen et al., 2011).

Metal composition

The profile for metals during summer is shown in **Fig. 5a**, Site D had the highest concentrations of Na and K. Al was lacking in all sites except site A. Ca is the only metal of natural origin that is absent in all sites. Mn was present in site B only while Zn is present in all sites. Other metals of anthropogenic origin were all lacking in all the sites. During winter, all metals of natural origin were present in all sites except Al which was absent in site A. Other than V, Mn, Zn, and Pb, other metals of anthropogenic origin were absent in all sites under investigation. The metallic elements in the $PM_{2.5}$ mostly exist in the solid phase and are distributed in the environment through atmospheric airflow or gravity sedimentation (Moreno et al., 2004). During summer, the metal composition accounted for an

274 average of 5.7% of the total mass of $PM_{2.5}$ in all the sites under investigation as shown in **Fig. 3**.
275 Specifically, Na has the highest composition, which is 35.2%, 25.1%, 45.9%, and 50.1% for sites A, B,
276 C, and D, respectively.

277 The predominance of Na in summer can be attributed to the sea salt droplets occasionally blown
278 by the westerly wind from the sea to the land surface. It is hypothesized that the main source of Fe is
279 re-suspension from the iron ore piles in the raw material storage site. Besides, during steel production,
280 ferromanganese (Fe-Mn), ferrosilicon (Fe-Si), and aluminium are added to remove excess oxygen. The
281 background soil of surrounding areas is rich in crustal elements such as Si, K, Mn, and Mg. The
282 northwest wind brings with it crustal elements and sea salt droplets. This is believed to cause high
283 concentrations of these crustal elements in $PM_{2.5}$. Zn metal accounted for between 6.39% and 10.5% of
284 the total mass of metals. The main source is believed to be the mobile sources in the sites of
285 investigation (Lin et al., 2020; Shen et al., 2020).

286 *Water-soluble ions*

287 In **Fig. 6**, the percentage composition of individual water-soluble ions is presented. During winter,
288 SO_4^{2-} was the most important component in all sites. In summer, NO_3^- was the most important
289 composition. The percentage composition of SO_4^{2-} was almost constant for the summer and winter
290 seasons. In all seasons and for all sites, SO_4^{2-}, NO_3^-, and NH_4^+.contributed about 90% of the total
291 water-soluble ions. The percentage composition of NH_4^+.in summer exceeded that of winter for all sites.
292 In winter, the water-soluble ionic components, SO_4^{2-} accounts for about 70% of the total water-soluble
293 ions by mass, followed by NH_4^+ with an average of 10%, and NO_3^- with an average of 5% ranked third,
294 as shown in **Fig. 3**. The predominance of SO_4^{2-} and NO_3^- implies that anthropogenic sources have a
295 higher contribution to ambient air $PM_{2.5}$ than natural sources. Information on the contribution of
296 primary and secondary emission sources to ambient air $PM_{2.5}$ can be obtained from the ratios of SO_4^{2-}
297 to NO_3^-. Further, as seen in **Table 4**, the percentage composition of SO_4^{2-} was significantly higher in
298 pile 1 compared to the other piles. This can be used to paint a picture of the transformation phenomena

299 of sulfate and nitrate ions (Colbeck and Harrison, 1984). Fine nitrate has been associated with aerosol
300 acidity and moisture content. Additionally, the oxygen isotopic anomalies of SO_4^{2-} and NO_3^-.in $PM_{2.5}$
301 are transferred to O_3 during the oxidation process of SO_2 an NO_x.

302 In **Fig. 7**, I and J values for summer and winter for the four sites are presented. For all sites, I and
303 J values exceeded the threshold during winter. On the other hand, they fell below the threshold during
304 winter. The main constituents of secondary derived inorganic salts in the atmosphere NH_4^+, NO_3^-. and
305 SO_4^{2-}, easily exist in the air as NH_4NO_3, NH_4HSO_4, $(NH_4)_2SO_4$, and other salt types. Previously, it was
306 pointed out that I is the equivalent concentration ratio of ammonium and sulfate (Seinfeld et al., 1998).
307 When the value of $I \geq 2$, it implies that SO_4^{2-} has been neutralized and mainly exists as $(NH_4)_2SO_4$. On
308 the other hand, if $I < 2$ then only part of it exists as $(NH_4)_2SO_4$, and free sulfate ions still exist in the
309 atmosphere.

$$\mathrm{I} = \frac{NH_4^+{}_{eq}}{SO_4^{2-}{}_{eq}} \qquad (2)$$

310 The 24-hour ratio of NH_4^+ to NO_3^- and SO_4^{2-} ratio is represented by the J value (Chu, 2004). When
311 $J < 1$, then NH_4^+ is insufficient to neutralize NO_3^- and SO_4^{2-} and therefore, they are acidic. On the
312 other hand, if J>1, NH_4^+ is in surplus, and NO_3^- and SO_4^{2-} are basic.

$$\mathrm{J} = \frac{NH_4^+{}_{eq}}{2 \times SO_4^{2-}{}_{eq} + NO_3^-{}_{eq}} \qquad (3)$$

313 Herein, the value of I ranged between 0.81and 1.30 while the J value ranged between 0.37- 0.60,
314 I<2, J<1, indicating the presence of NO_3^- and SO_4^{2-} and an acidic atmosphere.

315 From **Table 4**, the percentage composition of SO_4^{2-} was significantly higher in pile 1 compared to
316 the other piles. Further, water-soluble ions formed the most important component in the limestone piles
317 especially, SO_4^2, Ca^{2+}. All these led to a lower value of both I and j ratios. While the percentage
318 composition of SO_4^{2-} in total $PM_{2.5}$ coal pile 1 exceeded 50%, that is the other coal piles barely reached

10%. This suggests that the contribution of coal piles to secondary aerosols could be highest in coal pile-1.

Carbon content

From **Fig. 4**, the mass of organic carbon exceeded elemental carbon at all sites under investigation and during all seasons. The $\frac{OC}{EC}$ ratios for the four sites are presented in **Table 3**, where sites A and D had the highest values during summer. Carbon was a minor component in the iron ore pile as shown in **Table 4**. Organic carbon exceeded elemental carbon in all piles except the third iron pile. Unlike in the iron ore piles, carbon was the major component in the coal piles. The percentage composition of elemental carbon exceeded that of organic carbon in all piles except the second pile. The percentage composition of elemental carbon was more than 20% except in the first coal pile where it was about 2%. The percentage composition of carbon in the coal pile-1 can be associated with high sulfate concentrations. The high sulphate content is hypothesized to originate from leaching of overlying steel slags.

As seen in **Table 4**, carbon content was the second most dominant composition in the limestone piles with the OC more abundant compared to EC (Tseng et al., 2019). Only three metal types were present in significant percentage compositions in the three stone piles including Mg, Ca, and Fe. The other metal compositions were either insignificant or non-existent. As seen in **Table 4**, EC formed a significant percentage composition of the sinter pile with about 21%. The rest of the compositions had less than 5% of the percentage composition. In the coke pile, OC exceeded EC unlike in the sinter pile. The carbon component accounts for 17.4% of the total mass, whereby OC exceeds EC. The pollution source may have come from organic carbon derived from photochemical reactions or pollution emissions such as industrial combustion (Hays et al., 2005).

Chemical fingerprints for the $PM_{2.5}$ in the raw material piles

From **Table 4**, the chemical profiles of different types of iron ore piles are presented. As anticipated Fe content from the iron pile ranged from 14.8 to 46.3% and hence the most abundant species in all the 5 iron piles. Coal pile-1 had a significant component of Na, Al, Si, K, and Fe. The percentage composition of all metals was less than 10% in all the 5 iron piles except Fe in core pile-1which was 14.4%. The percentage composition of metals in the other piles was either non-existent or insignificant. Additionally, the iron piles had water-soluble ions and other crustal components. Among the water-soluble ions, SO_4^{2-} was present in the highest concentration. In Iron pile -1, it was 22% while in the other piles it ranged between 4 and 6%. Aluminium was present in the highest percentage for iron pile-1, while in the other piles, it was less than 2%. The crustal elements included Na, Mg, Al, K, and Si, while the water-soluble ions included 4 anionic species such as SO_4^{2-}, NO^-, CI^-, F^-, and 5 cationic species including Na^+, K^+, Ca^{2+}, Mg^{2+}, NH_4^+. Among the water-soluble ions, SO_4^{2-} was the most abundant water-soluble ion accounting for (4.2~22%) in all piles. OC content was highest in Iron pile-1 at 11.3% while in the other iron piles, it ranges between 4.7~9.1%. This is suspected to contribute to the ambient air $PM_{2.5}$ through re-suspension especially during the sea-land breeze associated with moments of no precipitation in winter (Cao et al., 2008).

The composition of coal pile-1 as presented in **Table 4** differed from the other coal piles. Its main component which is SO_4^{2-} contributed 55.3% of all the water-soluble ions. The metal composition is 31.6% while that of carbon is 6.45%. The carbon content is high in the other four coal piles. In coal pile -2, organic carbon (28%) exceeded the elemental carbon (20.1%) unlike in the other coal piles. As anticipated, in the other coal piles, the elemental carbon exceeded the organic carbon (Moreno et al., 2004; Fang et al., 2008). The elemental carbon ranged between 25.4~ 41.9% while the organic carbon ranged between 9.06~ 10.8%. Water-soluble ions accounted for between 11.4~12.0% whereby SO_4^{2-} was responsible for 9.62~11.4%. The metal composition was 6.32~8.51% while the contribution from crustal elements was insignificant. As seen in **Table 4**, Ca^{2+} and Fe formed the highest percentage

366 composition of the sinter pile with about 20% each (Moreno et al., 2004; Fernández-González et al.,
367 2017). One possible reason for high Ca^{2+} is the contamination of the sinter pile with dust from the
368 limestone pile which naturally has high concentrations of Ca^{2+}. Additionally, Within an integrated steel
369 plant, the presence of Oxygen species during reduction and refining processes causes the expulsion of
370 low molecular weight metals in the form of fine particulates. Further, the leaching of steel slags for
371 long periods could also explain the high Ca^{2+} concentration.

372 In the limestone pile, the three piles differed significantly in terms of chemical composition. In
373 limestone pile-1, total carbon accounted for 35.9% while metals accounted for 17%. Specifically,
374 elemental carbon was 10.6 % while organic carbon was 25.3 %. For the metal composition,
375 Magnesium and calcium accounted for .9.86% and 4.19% respectively. Water-soluble ions accounted
376 for 13.2 % whereby the individual contribution from Ca^{2+}, SO_4^{2-}, and Mg^{2+} were 6.64%, 3.86%, and
377 2.54% respectively. In limestone pile-2, water-soluble ions were the main chemical composition where
378 Ca^{2+} and SO_4^{2-} accounted for 18.9% and 4.93% respectively. Metals and carbon accounted for 16.4%
379 and 15.6% respectively. Specifically, the organic carbon accounted for 13.9%. Stone pile-3 had water-
380 soluble ions as the main components, just like stone pile-2. They accounted for 47.7% of the total
381 chemical composition with SO_4^{2-} accounting for 39.5%. Carbon accounted for 20.2% while metal
382 contributed 3.13%. As anticipated, Ca^{2+} was among the major components in limestone and could have
383 contributed Ca^{2+} in the ambient air $PM_{2.5}$ after re-suspension (Monshi and Asgarani, 1999).

384 The main chemical component in the coke pile is carbon and it accounted for 27.4%. Water-
385 soluble ions and metal accounted for 21.7% and 11.6% respectively. Specifically, SO_4^{2-}, K^+, and Ca^{2+}
386 contributed 11.4%, 6.58%, and 3.18% respectively whereas Fe, Si, and Al accounted for 6.07%, 4.19%,
387 and 0.89%. For the sinter pile, the metal component was the most important accounting for 37.4%.
388 Specifically, the contribution from Fe, Ca, K, Si, Al, Na, and Mg were 18.6%, 5.69, 2.51, 2.24, 2.16,
389 1.91, and 1.08% respectively. $PM_{2.5}$ from the coal mine has less density compared to the other raw
390 material piles and hence had a wider range of diffusion. The $PM_{2.5}$ from limestone and iron ore are

391 characterized by high density and thus smaller diffusion distances from the raw material piles to
392 adjacent locations (Moreno et al., 2004; Cohen et al., 2011).
393 *Contribution of various pollution sources from the receptor model (CMB)*
394 The results of seasonal variation and fingerprint data for pollution sources are summarized in
395 **Table 5**. From the compositional analysis, the main sources of $PM_{2.5}$ in the neighborhood of the raw
396 material storage field are hypothesized as, petrochemical plants, boilers, background soil dust,
397 secondary sources of sulfates and nitrates, and combustion sources. During winter, the main pollution
398 sources of $PM_{2.5}$ for site A, B, and C are, petrochemical industry, NO_3^-, and SO_4^{2-} where they formed
399 20.6%, 18.5%, and 12.4%; 22.8%, 17.0%, and 10.6%; and 17.8%, 17.4%, and 13.9% respectively.
400 Those of site D are NO_3^- (19.4%), boiler combustion (18.0 %), derived sulfate (13.3%), and soil dust
401 (11.8%). Secondary nitrate (NO_3^-) were mostly from mobile sources and other combustion sources
402 upstream (Yang et al., 2019). Ammonium released from fertilizers and animal feeds is also believed to
403 have contributed to high concentrations of nitrates and sulfates in $PM_{2.5}$.The petrochemical industry
404 was dominant in sites A, B and C because of their proximity to the petroleum products processing
405 plant. In addition to nitrates and sulfates, the boiler and background soil were dominant ambient $PM_{2.5}$
406 sources in site D due to the dominating influence of the land-sea breeze and lack of rainfall (Lee et al.,
407 2008; Yuan et al., 2018).
408 The average contribution of the major pollution sources during summer for
409 site A includes sulfate (28.70%), traffic Source (16.36%), soil dust (13.38%); those for site B includes
410 sulfate (43.47%) and traffic sources (13.74%); for site C they are derived sulfate (36.95%), traffic
411 source (14.19%), and derived organic carbon (13.85%); while those for site D includes sulfate
412 (35.34%), soil dust (27.44%), and organic carbon (14.91%). Overall, secondary aerosols are the
413 predominant part of $PM_{2.5}$ in the area under investigation. Site A is predominantly affected by the west
414 wind and northwest west wind. The petrochemical emissions source is located on the west side of the
415 raw material storage site. Through CMB, it was established that emissions from the petrochemical

plant, boiler, and incinerator flow towards the raw material storage site leading to an increase in the ambient air sulfate concentration (Hu et al., 2019). At site B, during summer, the station is affected by the northwest west wind, and south wind, bringing sea droplets to the station. At site C, sea salt droplets are the main source of pollution under the influence of the sea and land breeze. Site D has no obvious pollution source during summer except mobile sources which lead to amplified nitrate composition in their $PM_{2.5}$. At site D, the crustal composition, as well as the contribution from mobile sources, are the predominant compositions of $PM_{2.5}$. Additionally, it is adjacent to the petrochemical plant and therefore, under the influence of west, southwest, and northeast winds as well as the land-sea breezes (Cohen et al., 2004; Fang et al., 2018). The dominance of sulfates and secondary OC in summer for all sites indicates active biogenic sources in the neighborhood.

Conclusions

The main goal of these investigations was to establish the contribution of a raw material storage site to ambient air $PM_{2.5}$ in the surrounding area. The major chemical compositions of resuspended $PM_{2.5}$ from iron ore, coal, limestone, coke, and sinter piles were successfully investigated. Chemical composition differed between different piles. Further, there were slight variations among piles with the same key compositions. The variation in the concentration of $PM_{2.5}$ between the two seasons indicates that prevailing weather conditions such as dominant wind direction, temperature, and rainfall significantly affected the $PM_{2.5}$ concentrations. Lower wind intensities in winter as compared to summer led to inadequate circulations of air masses and hence elevated concentrations of $PM_{2.5}$ within the site of investigation during winter. In the summer, the $PM_{2.5}$ concentration is between 13.7-18 μg m^{-3}, and water-soluble ions account for 54.2% of the total. The main ambient $PM_{2.5}$ components are SO_4^{2-} (73.6%), NH_4^+ (13.7%) and NO_3^- (7.45%). In winter, the $PM_{2.5}$ ranged between 44.7 and 48.0 μg m^{-3}, and water-soluble ions account for 49.2% of the $PM_{2.5}$ total mass. The main components are NO_3^- (36.5%), SO_4^{2-} (30.1%) and NH_4^+ (24.3%). In the winter, the relative humidity (above 70%) and the

low-temperature environment lead to high ambient air NO_3^- concentration. The site for material storage has a more obvious impact on the regions downwind. The $\frac{OC}{EC}$ ratios indicated that the predominant sources for ambient air $PM_{2.5}$ were photochemical, industrial and combustion processes. However, the surroundings of the raw material storage site are affected more by other notable pollution sources including petrochemical plants, soil dust, derived sulfates and nitrates, and mobile sources. The dominance of secondary organic aerosols raises concerns about the importance of dealing with the emission of secondary aerosol precursors.

References

Ahmad, T., Park, J., Keel, S., Yun, J., Lee, U., Kim, Y. and Lee, S.-S. (2018). Behavior of Heavy Metals in Air Pollution Control Devices of 2,400 Kg/H Municipal Solid Waste Incinerator. *Korean J. of Chem. Eng.* 35: 1823-1828.

Artíñano, B., Salvador, P., Alonso, D.G., Querol, X. and Alastuey, A. (2003). Anthropogenic and Natural Influence on the Pm10 and Pm2. 5 Aerosol in Madrid (Spain). Analysis of High Concentration Episodes. *Environ Poll.*125: 453-465.

Bell, M.L., Ebisu, K., Leaderer, B.P., Gent, J.F., Lee, H.J., Koutrakis, P., Wang, Y., Dominici, F. and Peng, R.D. (2014). Associations of Pm2. 5 Constituents and Sources with Hospital Admissions: Analysis of Four Counties in Connecticut and Massachusetts (USA) for Persons≥ 65 Years of Age. *Environ. Health Persp.* 122: 138-144.

Benchrif, A., Guinot, B., Bounakhla, M., Cachier, H., Damnati, B. and Baghdad, B. (2018). Aerosols in Northern Morocco: Input Pathways and Their Chemical Fingerprint. *Atmos Environ* 174: 140-147.

Cao, J.J., Chow, J.C., Watson, J.G., Wu, F., Han, Y.M., Jin, Z.D., Shen, Z.X. and An, Z.S. (2008). Size-Differentiated Source Profiles for Fugitive Dust in the Chinese Loess Plateau. *Atmos. Environ.* 42: 2261-2275.

Chalupa, D.C., Morrow, P.E., Oberdörster, G., Utell, M.J. and Frampton, M.W. (2004). Ultrafine Particle Deposition in Subjects with Asthma. *Environ Health Persp* 112: 879.

Chen, C.-S. and Chen, Y.-L. (2003). The Rainfall Characteristics of Taiwan. *Monthly Weather Review* 131: 1323-1341.

Choi, L.-T., Tu, J., Li, H. and Thien, F. (2007). Flow and Particle Deposition Patterns in a Realistic Human Double Bifurcation Airway Model. *Inhal. Toxicol.* 19: 117-131.

Chu, S.-H. (2004). Pm2.5 Episodes as Observed in the Speciation Trends Network. *Atmos. Environ.* 38: 5237-5246.

Cohen, D.D., Garton, D., Stelcer, E., Hawas, O., Wang, T., Poon, S., Kim, J., Choi, B.C., Oh, S.N., Shin, H.J., Ko, M.Y. and Uematsu, M. (2004). Multielemental Analysis and Characterization of Fine Aerosols at Several Key Ace-Asia Sites. *J of Geophysl. Res.-Atmos.* 109.

Cohen, D.D., Stelcer, E., Garton, D. and Crawford, J. (2011). Fine Particle Characterisation, Source Apportionment and Long-Range Dust Transport into the Sydney Basin: A Long Term Study between 1998 and 2009. *Atmos. Poll. Res.* 2: 182-189.

Colbeck, I. and Harrison, R.M. (1984). Ozone—Secondary Aerosol—Visibility Relationships in North-

West England. *Sci. of the Tot. Environ.* 34: 87-100.
Cullen, J.M., Allwood, J.M. and Bambach, M.D. (2012). Mapping the Global Flow of Steel: From Steelmaking to End-Use Goods. *Environ. Sci. & Tech.* 46: 13048-13055.
de la Campa, A.M.S., de la Rosa, J.D., Gonzalez-Castanedo, Y., Fernandez-Camacho, R., Alastuey, A., Querol, X. and Pio, C. (2010). High Concentrations of Heavy Metals in Pm from Ceramic Factories of Southern Spain. *Atmos. Res.* 96: 633-644.
Dejmek, J., Selevan, S.G., Benes, I., Solanský, I. and Srám, R.J. (1999). Fetal Growth and Maternal Exposure to Particulate Matter During Pregnancy. *Environ. Health. Persp*. 107: 475-480.
Fang, G.-C., Wu, Y.-S., Chou, T.-Y. and Lee, C.-Z. (2008). Organic Carbon and Elemental Carbon in Asia: A Review from 1996 to 2006. *J of Haz. Mat.* 150: 231-237.
Fang, J., Fan, J.M., Lin, Q., Wang, Y.Y., He, X., Shen, X.D. and Chen, D.L. (2018). Characteristics of Airborne Lead in Hangzhou, Southeast China: Concentrations, Species, and Source Contributions Based on Pb Isotope Ratios and Synchrotron X-Ray Fluorescence Based Factor Analysis. *Atmos. Poll. Res.* 9: 607-616.
Feng, J., Yu, H., Liu, S., Su, X., Li, Y., Pan, Y. and Sun, J. (2016). Pm2. 5 Levels, Chemical Composition and Health Risk Assessment in Xinxiang, a Seriously Air-Polluted City in North China. *Environ. Geochem. and Health*: 1-13.
Fernández-González, D., Ruiz-Bustinza, I., Mochón, J., González-Gasca, C. and Verdeja, L.F. (2017). Iron Ore Sintering: Process. *Mineral Proces. and Extrac. Metallurg. Review* 38: 215-227.
Hays, M.D., Fine, P.M., Geron, C.D., Kleeman, M.J. and Gullett, B.K. (2005). Open Burning of Agricultural Biomass: Physical and Chemical Properties of Particle-Phase Emissions. *Atmos. Environ.* 39: 6747-6764.
Houck, J.E. (1991). Source Sampling for Receptor Modeling, In *Rec. Model for Air Qual. Mgt.*, Elsevier Amsterdam, pp. 57-65.
Hu, J., Wang, H., Zhang, J., Zhang, M., Zhang, H., Wang, S. and Chai, F. (2019). Pm2. 5 Pollution in Xingtai, China: Chemical Characteristics, Source Apportionment, and Emission Control Measures. *Atmos.* 10: 121.
Lai, I.-C. and Brimblecombe, P. (2020). Long-Range Transport of Air Pollutants to Taiwan During the Covid-19 Lockdown in Hubei Province. *Aerosol Air Qual. Res.* 20.
Lee, S.W., Herage, T., He, I. and Young, B. (2008). Particulate Characteristics Data for the Management of Pm2.5 Emissions from Stationary Combustion Sources. *Powder Technol.* 180: 145-150.
Lin, C.-H., Wu, Y.-L., Lai, C.-H., Watson, J.G. and Chow, J.C. (2008). Air Quality Measurements from the Southern Particulate Matter Supersite in Taiwan. *Aerosol Air Qual. Res.* 8: 233-264.
Lin, Y.-C., Li, Y.-C., Amesho, K.T.T., Chou, F.-C. and Cheng, P.-C. (2020). Filterable Pm2.5, Metallic Elements, and Organic Carbon Emissions from the Exhausts of Diesel Vehicles. *Aerosol Air Qual. Res.* 20: 1319-1328.
Loo, B.W., Jaklevic, J.M. and Goulding, F.S. (1975). Dichotomous Virtual Impactors for Large Scale Monitoring of Airborne Particulate Matter. *Fine Particles (ed. by BYH LIU)*: 311-350.
Monshi, A. and Asgarani, M.K. (1999). Producing Portland Cement from Iron and Steel Slags and Limestone. *Cement and Concrete Res.* 29: 1373-1377.
Moreno, T., Merolla, L., Gibbons, W., Greenwell, L., Jones, T. and Richards, R. (2004). Variations in the Source, Metal Content and Bioreactivity of Technogenic Aerosols: A Case Study from Port Talbot, Wales, Uk. *Sci. of the Tot. Environ.* 333: 59-73.
Nogueira, J.B. (2009). Air Pollution and Cardiovascular Disease. *Portuguese J of cardiol: an official J of the Portuguese Soc. of Cardiol.* 28: 715.
Pace, T.G. (1991). Receptor Modeling in the Context of Ambient Air Quality Standard for Particulate Matter, In *Rec. Model for Air Qual. Mgt., Data Handling in Sci. and Tech.*, Elsevier Amsterdam, pp. 255-297.

Pandis, S.N., Harley, R.A., Cass, G.R. and Seinfeld, J.H. (1992). Secondary Organic Aerosol Formation and Transport. *Atmos Environ. Part A. General Topics* 26: 2269-2282.
Pöschl, U. (2005). Atmospheric Aerosols: Composition, Transformation, Climate and Health Effects. *Angewandte Chem Intern Edition* 44: 7520-7540.
Seinfeld, J.H., Pandis, S.N. and Noone, K. (1998). Atmospheric Chemistry and Physics: From Air Pollution to Climate Change. *PhT* 51: 88.
She, H., Cheng, P.-H., Yuan, C.-S., Yang, Z.-M. and Ie, I.-R. (2020). Chemical Characteristics, Spatiotemporal Distribution, and Source Apportionment of Pm2. 5 Surrounding Industrial Complexes in Southern Kaohsiung. *Aerosol and Air Qual. Res.* 20: 557-575.
Shen, H.Z., Yang, T.M., Lu, C.C., Yuan, C.S., Hung, C.H., Lin, C.T., Lee, C.W., Ling, G.H., Hu, G.R. and Lo, K.C. (2020). Chemical Fingerprint and Source Apportionment of Pm2.5 in Highly Polluted Events of Southern Taiwan. *Environ. Sci. and Poll. Res.* 27: 6918-6935.
Tsai, S.-S., Goggins, W.B., Chiu, H.-F. and Yang, C.-Y. (2003). Evidence for an Association between Air Pollution and Daily Stroke Admissions in Kaohsiung, Taiwan. *Stroke* 34: 2612-2616.
Tseng, Y.L., Yuan, C.S., Bagtasa, G., Chuang, H.L. and Li, T.C. (2019). Inter-Correlation of Chemical Compositions, Transport Routes, and Source Apportionment Results of Atmospheric Pm2.5 in Southern Taiwan and the Northern Philippines. *Aerosol and Air Qual. Res.* 19: 2645-2661.
Virtanen, A., Rönkkö, T., Kannosto, J., Ristimäki, J., Mäkelä, J., Keskinen, J., Pakkanen, T., Hillamo, R., Pirjola, L. and Hämeri, K. (2006). Winter and Summer Time Size Distributions and Densities of Traffic-Related Aerosol Particles at a Busy Highway in Helsinki. *Atmos. Chem. and Phys.* 6: 2411-2421.
Wang, Y.-S., Chang, L.-C. and Chang, F.-J. (2020). Explore Regional Pm2. 5 Features and Compositions Causing Health Effects in Taiwan. *Environ. Mgt*: 1-16.
Weijers, E., Schaap, M., Nguyen, L., Matthijsen, J., Van Der Gon, H.D., Ten Brink, H. and Hoogerbrugge, R. (2011). Anthropogenic and Natural Constituents in Particulate Matter in the Netherlands. *Atmos. Chem. and Phys.* 11: 2281.
Wienke, D., Gao, N. and Hopke, P.K. (1994). Multiple Site Receptor Modeling with a Minimal Spanning Tree Combined with a Neural Network. *Environ. Sci. & Tech.* 28: 1023-1030.
Yang, H.-H., Dhital, N.B., Wang, L.-C., Hsieh, Y.-S., Lee, K.-T., Hsu, Y.-T. and Huang, S.-C. (2019). Chemical Characterization of Fine Particulate Matter in Gasoline and Diesel Vehicle Exhaust. *Aerosol Air Qual. Res.* 19: 1439-1449.
Yuan, C.S., Lu, C.C., Shen, H.Z. and Li, T.C. (2018). Metallic Characteristics of Pm2.5 and Pm2.5-10 for Clustered Aeolian Dust Episodes Occurred in an Extensive Fluvial Basin During Rainy Season. *J. of the Air & Waste Mgt. Assoc.* 68: 1085-1102.
Zhang, L., Wang, F., Ji, Y., Jiao, J., Zou, D., Liu, L., Shan, C., Bai, Z. and Sun, Z. (2014). Phthalate Esters (Paes) in Indoor Pm10/Pm2. 5 and Human Exposure to Paes Via Inhalation of Indoor Air in Tianjin, China. *Atmos. Environ.* 85: 139-146.
Zhao, J., Gao, Z., Tian, Z., Xie, Y., Xin, F., Jiang, R., Kan, H. and Song, W. (2013). The Biological Effects of Individual-Level Pm2. 5 Exposure on Systemic Immunity and Inflammatory Response in Traffic Policemen. *Occupat. and Environ. Med.* 70: 426-431.
Zhao, Y., Cui, K., Chen, S., Yin, Z., Chao, H.-R. and Chang-Chien, G.-P. (2018). Atmospheric Pm2. 5, Total Pcdd/Fs-Who2005-Teq Level and Wet Deposition: Cases of Jinan and Weihai Cities, China. *Aerosol Air Qual. Res.* 18: 3081-3095.

571 **Table 1** Precision and stability of element analyzer

Carrier gas	Accuracy	Precision
Helium	≦ 0.3%	≦ 0.2%
Argon	≦ 0.5%	≦ 0.4%

572

573 **Table 2** Operating conditions of element analyzer

Process	Set conditions
Oxidation furnace temperature (°C)	1020
Reduction furnace temperature (°C)	500
Carrier gas flow rate (mL min^{-1})	100
Sample delay time (s)	8-15
Total execution time (min)	9-12

574

575 **Table 3** The concentrations of OC and EC and the OC/EC

	Site A		Site B		Site C		Site D	
	Summer	Winter	Summer	Winter	Summer	Winter	Summer	Winter
OC (μg m^{-3})	3.00	6.20	1.20	5.80	2.30	5.60	2.30	5.90
EC (μg m^{-3})	1.80	1.70	0.80	2.30	1.20	2.20	0.60	1.80
OC/EC	1.70	3.61	1.48	2.56	1.93	2.50	4.04	3.28

576

577

578 **Table 4** Percentage masses of individual components in each pile of raw material

	Raw materials														
	Iron piles					Coal piles					Limestone piles			Coke pile	Sinter pile
	IP1 (%)	IP2 (%)	IP3 (%)	IP4 (%)	IP5 (%)	CP1 (%)	CP2 (%)	CP3 (%)	CP4 (%)	CP5 (%)	LP1 (%)	LP2 (%)	LP3 (%)	(%)	(%)
Na	2.42	0.51	0.24	0.17	0.39	3.73	0.62	0.48	0.95	0.63	0.27	0.31	0.07	0.34	1.91
Mg	0.82	0.21	0.21	0.50	0.27	-	-	-	0.30	-	9.86	1.35	0.06	0.60	1.08
Al	7.54	0.46	1.39	2.07	2.06	2.03	0.64	1.09	1.24	0.95	0.30	0.46	0.09	0.89	2.16
Si	2.85	0.85	1.79	1.72	1.84	7.33	1.58	2.37	2.39	1.49	0.68	0.97	0.16	2.72	2.24
K	3.26	0.55	0.24	0.13	0.40	3.83	0.50	0.77	1.09	0.42	0.20	0.44	0.06	0.36	2.51
Ca	1.05	0.89	0.14	0.22	-	-	-	-	-	0.30	4.19	6.85	1.88	0.56	5.69
Ti	-	-	-	-	-	-	-	-	-	-	-	-	-	-	-
V	-	-	-	-	-	-	-	-	-	-	-	-	-	-	-
Cr	-	-	-	-	-	-	-	-	-	-	-	-	-	-	-
Mn	-	-	0.42	0.20	0.17	-	-	-	-	-	-	-	-	-	-
Fe	46.3	14.8	41.2	44.4	42.6	14.4	2.99	2.40	2.45	2.02	1.55	6.02	0.81	6.07	18.6
Co	-	-	-	-	-	-	-	-	-	-	-	-	-	-	-
Ni	-	-	-	-	-	-	-	-	-	-	-	-	-	-	-
Cu	-	-	-	-	-	-	-	-	-	-	-	-	-	-	-
Zn	-	-	-	-	-	-	-	-	-	0.50	-	-	-	-	0.19
As	-	-	-	-	-	-	-	-	-	-	-	-	-	-	-
Se	-	-	-	-	-	-	-	-	-	-	-	-	-	-	-
Sn	0.07	0.02	0.01	-	0.01	0.32	-	-	0.09	-	0.02	0.03	0.00	-	-
Cs	-	-	-	-	-	-	-	-	-	-	-	-	-	-	-
Pb	-	-	-	-	-	-	-	-	-	-	-	-	-	-	-
F^-	-	-	0.17	-	-	-	-	-	-	-	0.11	-	-	0.34	0.20
Cl^-	2.27	0.65	0.51	0.48	0.48	6.17	1.07	1.04	1.01	1.41	0.37	0.72	0.13	1.28	0.57
NO_3^-	1.27	0.23	0.34	0.27	0.31	2.68	0.59	0.70	0.80	0.59	0.17	0.31	0.06	0.51	0.34
SO_4^{2-}	22.7	5.83	4.63	4.19	6.59	55.3	10.8	11.1	9.62	11.4	3.86	4.93	39.5	11.41	5.85
Na^+	-	-	-	-	-	-	-	-	-	-	-	-	-	-	-
NH_4^+	-	-	-	-	-	-	-	-	-	-	-	-	-	-	-
K^+	-	-	-	-	-	-	-	-	-	-	-	-	-	6.58	-
Ca^{2+}	-	2.39	-	1.20	0.40	-	-	-	-	-	6.64	18.9	8.14	3.18	17.83
Mg^{2+}	-	-	-	-	-	-	-	-	-	-	2.54	-	-	-	-
OC	7.80	7.31	9.05	7.60	4.67	4.95	28.2	9.06	10.8	9.78	25.3	13.9	17.9	5.41	6.61
EC	2.40	0.95	11.3	0.00	0.08	1.50	20.1	25.4	39.8	41.9	10.6	1.73	2.24	22.0	2.73

Note: IP represents Iron piles
CP represents Coal piles
LP represents Limestone piles

579

580 **Table 5** Percentage contributions of $PM_{2.5}$ sources to the surrounding of the raw material storage site according to the chemical mass
581 balance

		Pollution sources																			
		I (%)	**II (%)**	**III (%)**	**IV (%)**	**V (%)**	**VI (%)**	**VII (%)**	**VIII (%)**	**IX (%)**	**X (%)**	**XI (%)**	**XII (%)**	**XIII (%)**	**XIV (%)**	**XV (%)**	**XVI (%)**	**XVII (%)**	**XVIII (%)**	**IXX (%)**	**XX (%)**	**Total (%)**
Winter	Site A	3.2	0.0	0.0	0.0	20.6	0.0	0.0	6.7	5.8	4.2	0.0	0.0	0.0	2.3	2.2	12.4	18.5	0.0	0.9	23.3	100
	Site B	4.4	7.4	0.0	0.0	22.8	0.0	0.0	5.1	0.8	6.2	0.0	0.0	0.0	2.4	1.6	10.6	17.0	0.0	0.7	20.9	100
	Site C	1.5	2.8	2.8	0.0	17.8	0.0	0.9	4.9	2.5	3.2	0.0	0.0	0.0	3.2	3.6	13.9	17.4	0.0	0.0	25.6	100
	Site D	0.0	0.0	0.0	0.0	2.8	0.0	18.0	7.0	0.0	0.0	0.0	0.0	0.0	11.8	1.5	13.2	19.3	8.9	1.1	16.4	100
Summer	Site A	0.3	3.1	0.0	0.0	9.6	0.0	0.0	16.4	3.6	0.0	0.0	0.0	0.0	13.4	3.8	28.7	2.6	9.2	0.0	9.4	100
	Site B	0.0	0.0	0.0	0.0	3.4	0.0	0.0	13.7	3.6	4.1	0.0	0.0	0.0	1.2	4.9	43.5	5.0	8.6	0.0	12.1	100
	Site C	0.0	0.0	0.0	0.0	0.0	0.0	0.0	14.2	0.0	0.0	0.0	0.0	0.0	18.9	6.8	36.9	3.0	13.8	0.0	6.4	100
	Site D	0.0	0.0	0.0	0.0	0.0	0.0	0.0	6.5	0.0	0.0	0.0	0.0	0.0	27.4	4.7	35.3	3.6	14.9	0.0	7.5	100

Note: I-Steel plant's converter, II-Coke Furnace, III- Sinter Furnace, IV- Electric Arc Furnace, V- Petrochemical Industry, VI- Incinerator, VII- Boiler, VIII- Traffic source, IX- Iron ore, X- Coal ore, XI- Stone ore, XII- Coke ore, XIII- Sinter ore, XIV- Soil dust, XV- Marine aerosol, XVI- Secondary sulfate, XVII- Secondary nitrate, XVIII- Secondary OC, IXX- Secondary EC, XX- Others

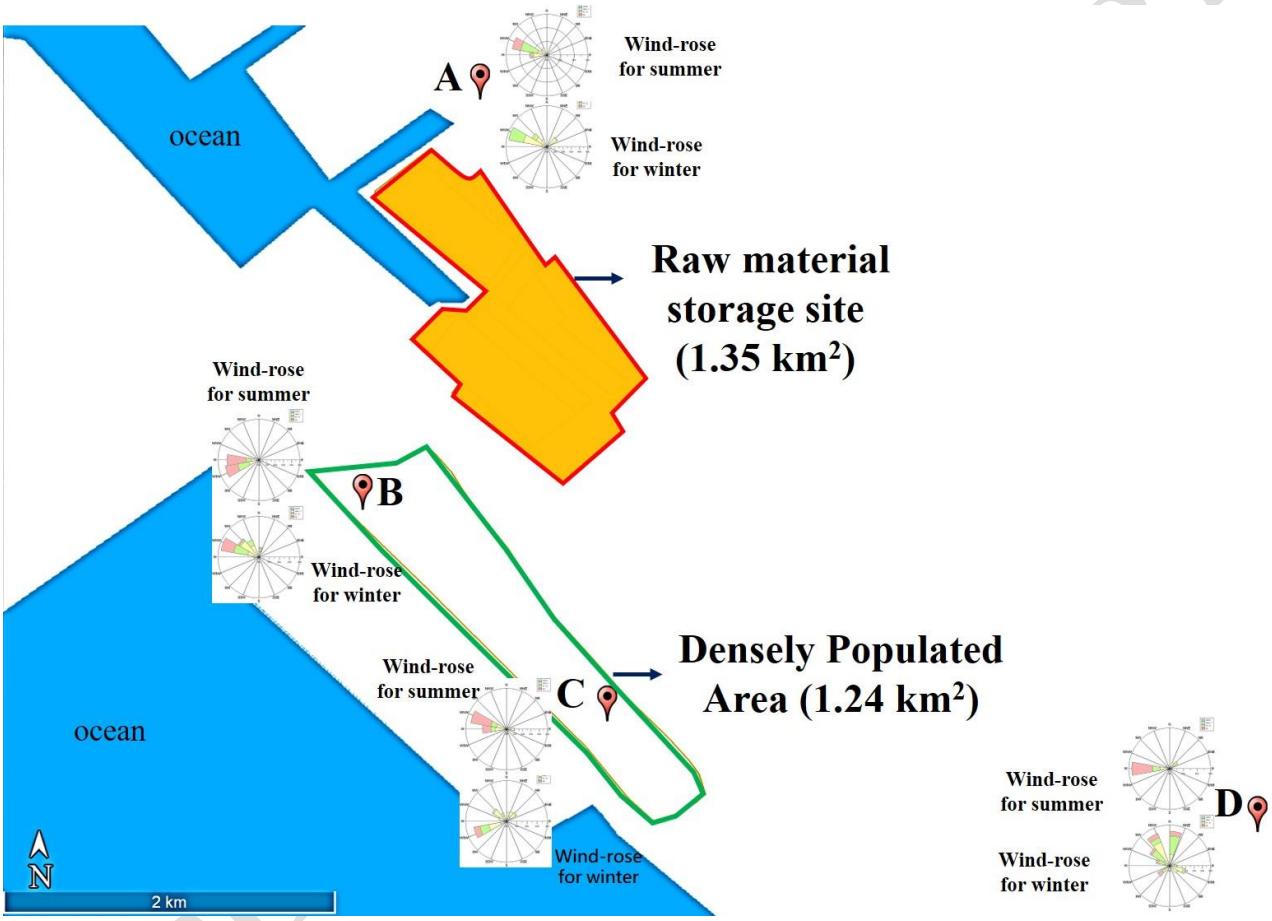

Fig. 1. A plan view of the raw material storage site in the area under investigations and the distribution of the sampling points for ambient air $PM_{2.5}$ including A, B, C, and D.

(a)

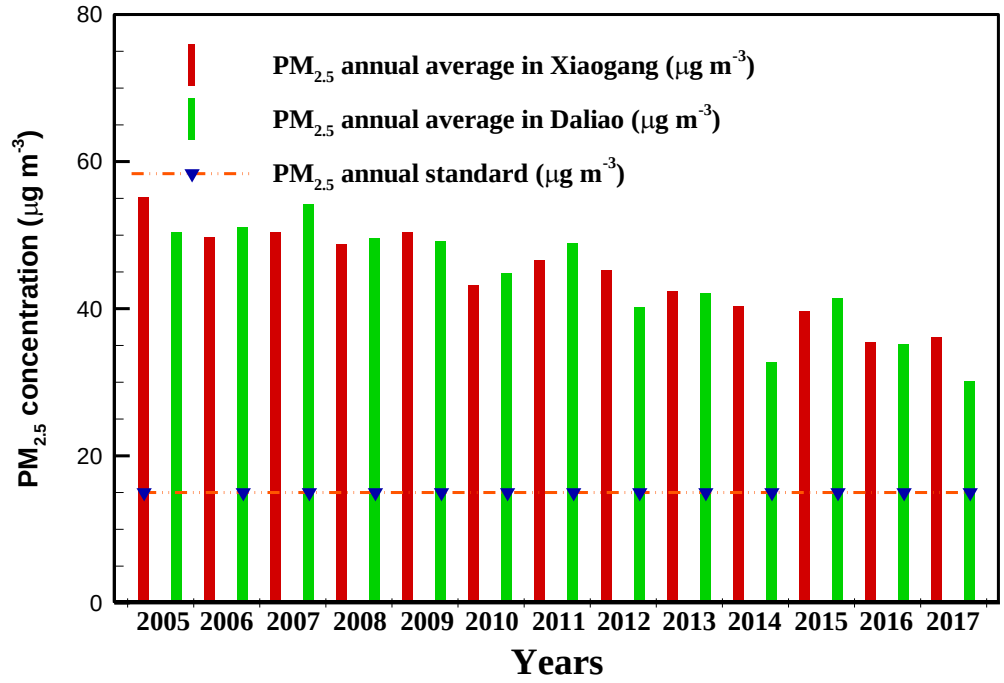

(b)

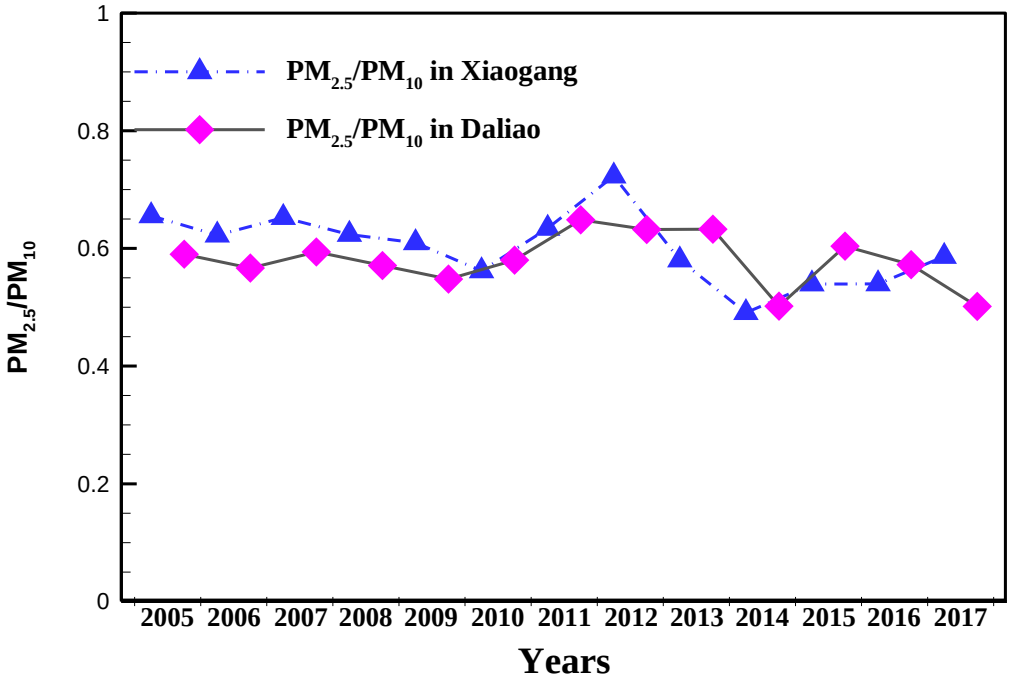

Fig. 2. Annual values for (a) ambient air PM2.5 concentrations and (b) $PM_{2.5}$ to PM_{10} ratios in Daliao and Xiaogang stations for the years 2005 to 2017.

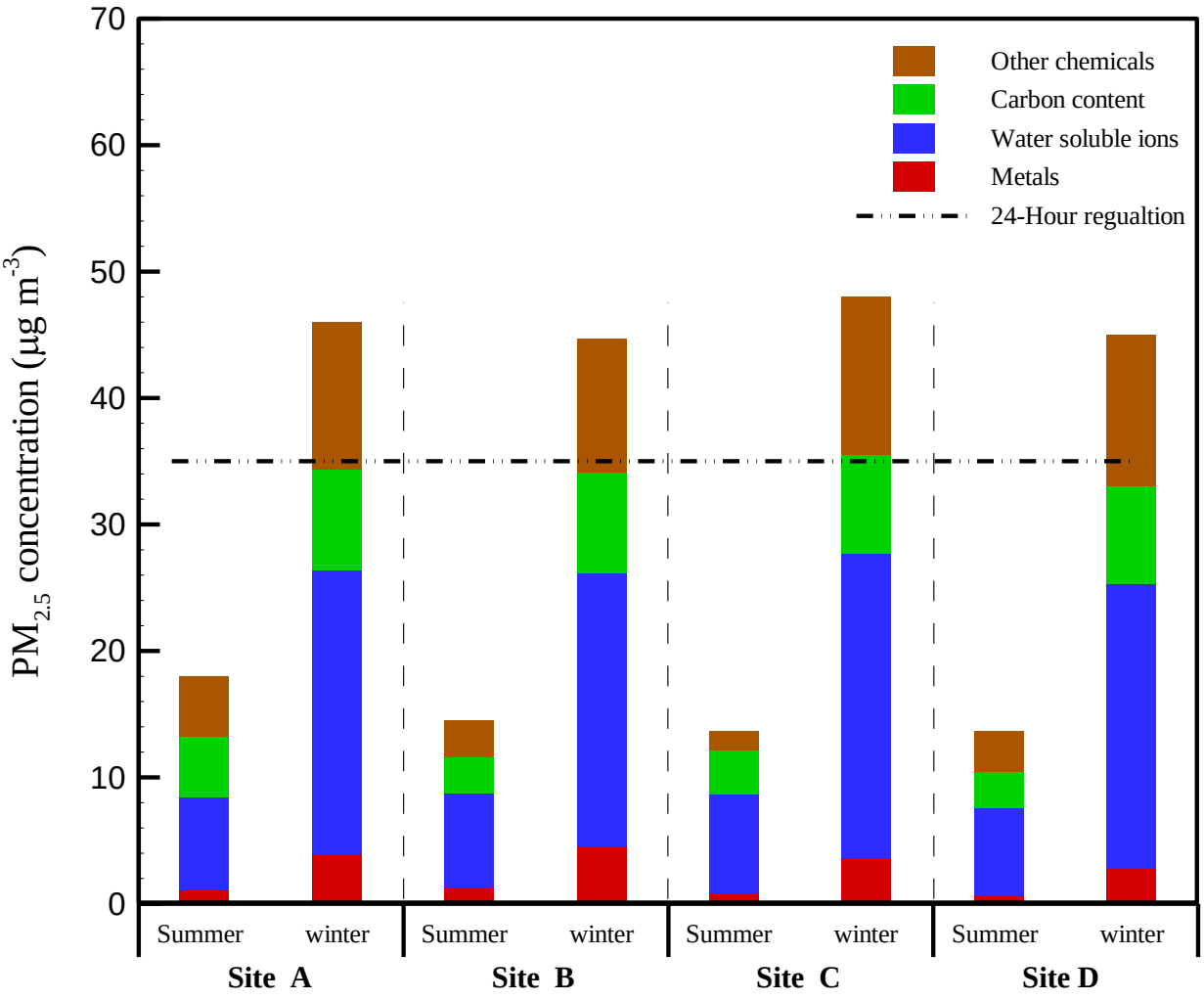

Fig. 3. The speciation of $PM_{2.5}$ during different seasons and at different sites of investigation.

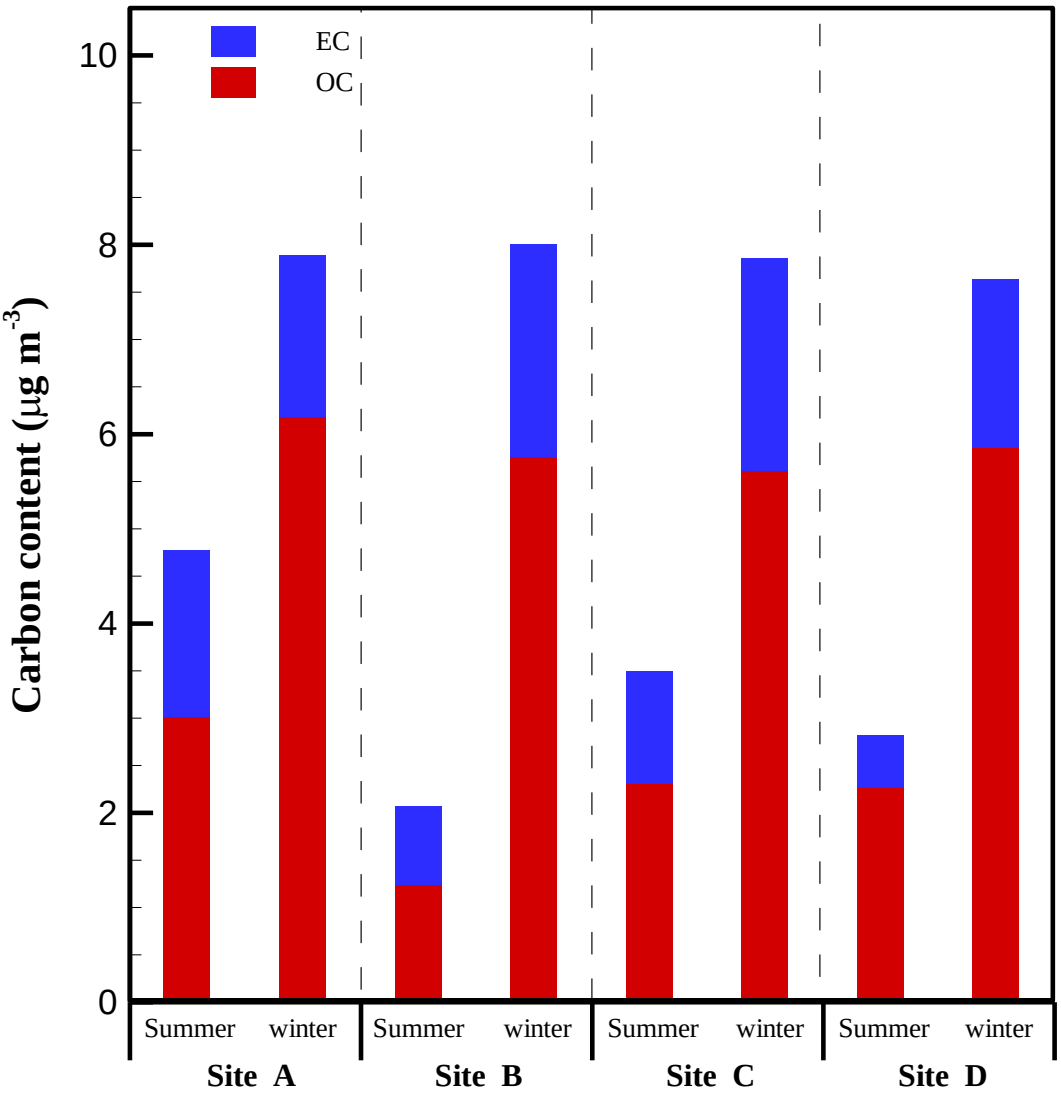

Fig. 4. Mass of elemental and organic carbon in $PM_{2.5}$ and the ratios of OC/EC for different sites during summer and winter.

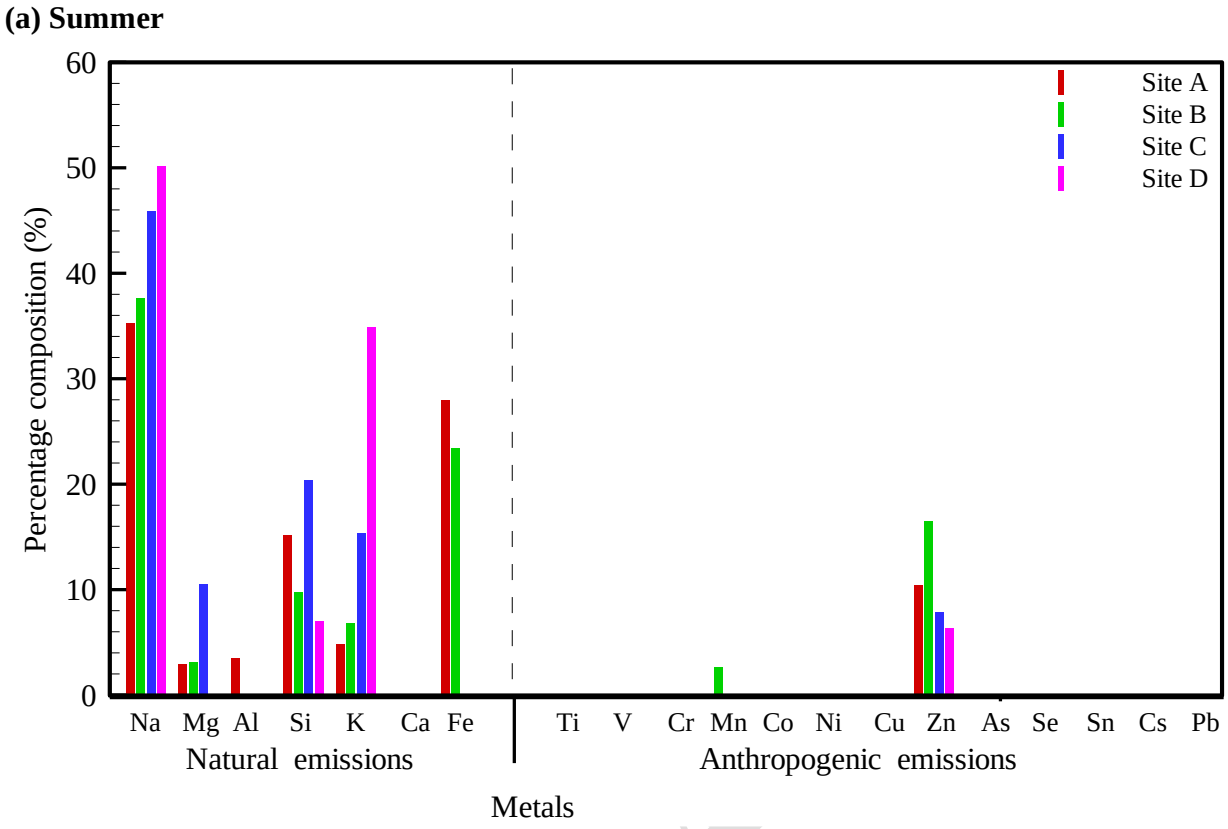

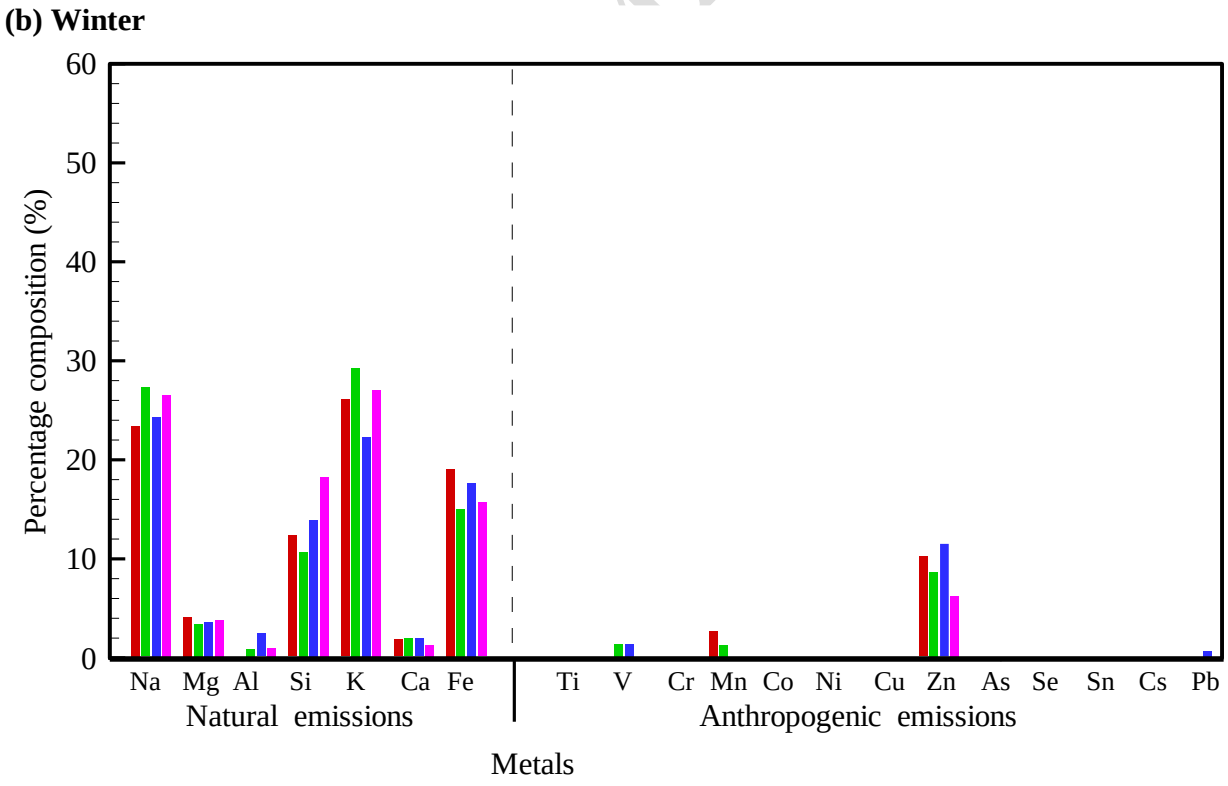

Fig. 5. $PM_{2.5}$ metal composition for sites A, B, C, and D during (a) summer (b) winter.

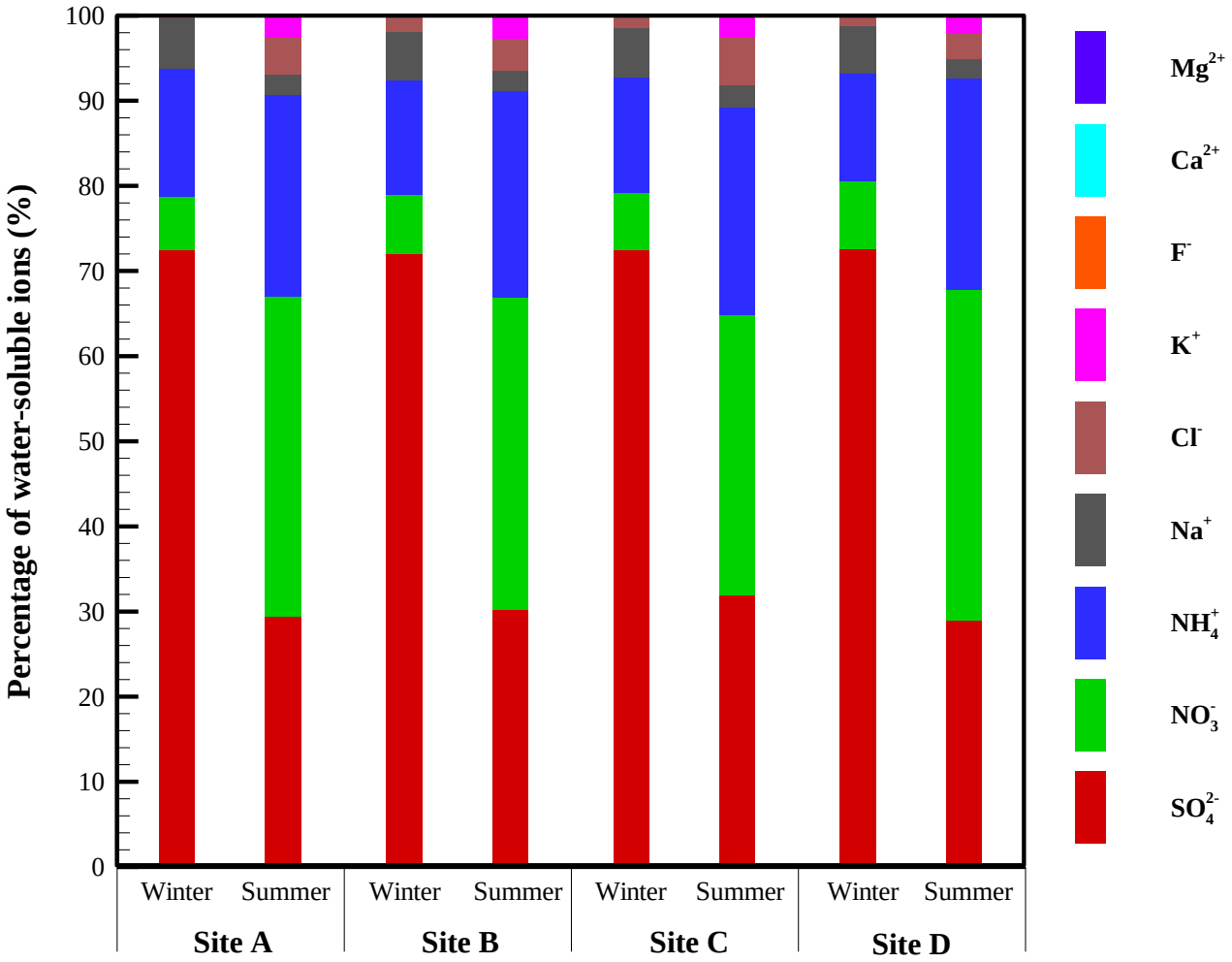

Fig. 6. Percentage of water-soluble ions in $PM_{2.5}$.for the seasons of winter and summer and at sites A, B, C, and D.

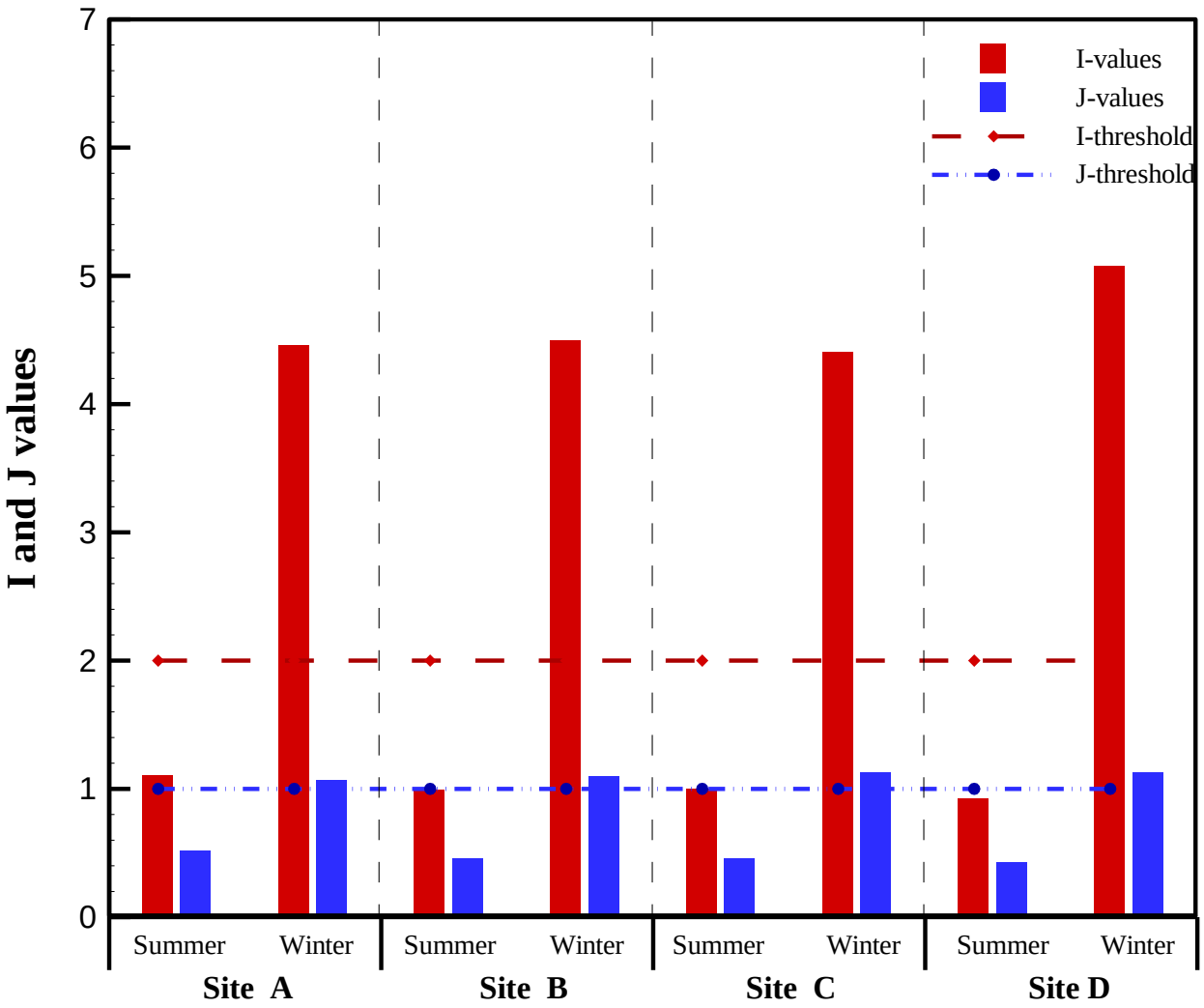

Fig. 7. I and J values for $PM_{2.5}$ and the thresholds in sites A, B, C, and D for summer and winter.